How long does it take a pyrite framboid to form?

David Rickard[1]

Graphical Abstract

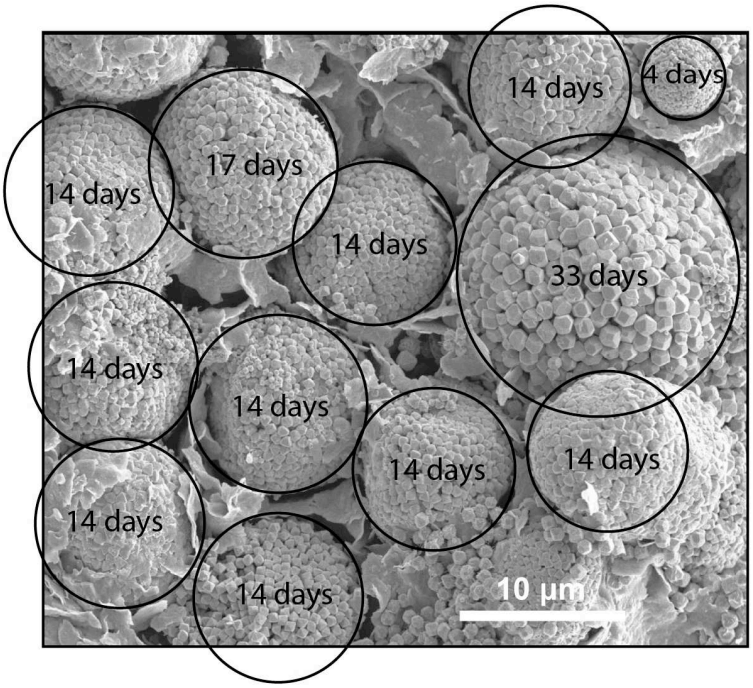

[1] School of Earth and Ocean Sciences, Cardiff University, CF10 3AT, Wales.

ABSTRACT

Framboids are defined as microscopic, sub-spheroidal clusters of equant and equidimensional microcrystals. The microcrystals are usually constituted of pyrite and framboidal pyrite is one of the most abundant mineral textures in the natural environment. They are of particular interest to geochemists, sedimentologists, paleobiologists and materials scientists because of their potential paleoenvironmental significance, their widespread involvement in fossilization and their potential for the manufacture of self-organizing materials. Here I use a simple diffusion-nucleation model to compute framboid formation times. The results show that pyrite framboids take between 3 hours and 3 years to form depending on framboid size. The time taken for the average sedimentary framboid to form is about 5 days and the average syngenetic framboid forms within 3 days. The shorter formation times for syngenetic compared with diagenetic framboids helps explain the smaller size relative size distributions of syngenetic framboids. This has led to the use of framboid size-frequency measurements as proxies for ancient euxinia. The relatively rapid formation of pyrite framboids explains how pyrite infills and preserves soft tissues before cell lysis and before deformation through burial has been initiated. One unexpected consequence of the model is that it further explains how commonly observed groups of framboids can form contemporaneously.

1 Introduction

Pyrite framboids (Fig. 1) may be one of the most abundant mineral textures on Earth: currently there may be up to about 10^{30} framboids on Earth or about 10^{9} times the number of sand grains (Rickard, 2015). At present they are forming at a rate of up to around 10^{14} per second. They form in a variety of environments from hydrothermal systems at temperatures of over 200^{o}C (Duckworth et al., 1994; Kanehira and Bachinski, 1967; Love and Amstutz, 1969; Read, 1968; Rickard and Zweifel, 1975) to euxinic water columns at less than 4^{o}C (Ross and Degens, 1974; Skei, 1988; Wilkin et al., 1996) and meromictic lakes (Perry and Pedersen, 1993). They are most abundant in sediments, however. Vallentyne (1963) for example, isolated 10^{5} framboids per gram dry sediment from a North American lake. They are found throughout the geologic column: the oldest reported framboids may be those from the late Archean (≤ 2.9 Ga) sediments of the Witwatersrand (Guy et al., 2010; Hallbauer, 1986).

[Figure 1]

Framboids were originally defined by Rust (1931) because they looked like microscopic raspberries (*framboise* in French). However the physical nature of pyrite framboids was not determined until this millennium. They are formed inorganically (Sweeney and Kaplan, 1973), although the sulfide is commonly biogenic (Large et al., 2001; MaClean et al., 2008; Rickard, 1969) and microbial biofilm may infiltrate the microarchitecture. The exceptional geometric organization displayed by some framboids reflects a classically forbidden, five-fold, crystal symmetry (Ohfuji and

Akai, 2002) and the individual microcrystals are not crystallographically aligned (Ohfuji et al., 2005; Ohfuji et al., 2006) even though they are often topologically organized in pseudo-crystalline arrangements. The process leading to the formation of framboids is free energy minimization through aggregation of the pyrite microcrystals under the influence of interfacial forces. The development of internal organization of microcrystals has been shown to be a subsequent structural modification resulting from entropy maximization in a spheroidal space (Wang et al., 2018).

That pyrite framboids can form rapidly in sediments has been known since earlier times. For example, Daubrée (1875) described globular pyrite in a Roman pavement and, more recently, pyrite framboids were observed in a dead newt (*Lissotriton vulgaris*) that had been trodden on by a miner's boot in an open pit in Ireland no more than a couple of years before (Rickard, 2012). Wilkin et al. (1996) used sedimentation rates to estimate that it took approximately 7 years to form a 25 μm framboid in Peru margin sediments and noted that, if crystal size distribution theory was applied to framboids, then a growth time of 0.4 years was indicated for syngenetic framboids in the Black Sea water column. Experimental syntheses of pyrite framboids and framboid-like textures also suggest that they form rapidly, within days to weeks (Ohfuji and Rickard, 2005). At this time, however, there has been no reported experimental study of the kinetics of pyrite framboid formation. In this paper, I address the question about how long it takes a pyrite framboid in sediments to form at ambient temperatures and pressures using a simple physical chemistry model.

2 Methods

2.1 Framboid formation

The characteristics of pyrite framboids are consistent with the LaMer model (Lamer, 1952; Lamer and Dinegar, 1950; Wilkin and Barnes, 1997) of nucleation and crystal growth (Fig. 2). This model is characterized by (1) a lag phase before nucleation becomes significant which can be regarded as the metastable phase zone width (Kashchiev, 2011), (2) burst nucleation (Baronov et al., 2015) where the rate of nucleation increases exponentially and may be completed in seconds and (3) a short growth phase where nucleation becomes again insignificant because of limitation in the supply of nutrients.

[Figure 2]

Burst nucleation was first defined as a key process in framboid formation by Read (1968) who realized that the similarity in size and habit of all the pyrite microcrystals in a framboid meant that they must have been formed at the same time. The lag phase in pyrite nucleation was observed as a reluctance of pyrite to nucleate in aqueous solutions (Schoonen and Barnes, 1991). Supersaturations of $> 10^{11}$ are required for pyrite to nucleate in aqueous solution even in the presence of an active surface (Rickard and Luther, 2007). Burst nucleation is then a consequence of these enormous levels of supersaturation. Once this critical supersaturation is reached, pyrite spontaneously nucleates, which causes a catastrophic decrease in the concentration of nutrients so that further nucleation is inhibited. The observation that pyrite framboids are formed more readily in environments where diffusive flow dominates, such as gels (Wang and Morse, 1996), organic matter (Papunen, 1966) and fine-grained

clastic sediments (Rickard, 2012), evidences the subsequent nutrient starvation that limits pyrite crystal growth. The final product is a myriad of pyrite microcrystals with similar habits and a limited size distribution.

The relative significance of diffusion-controlled growth in the development of the monodisperse microcrystals observed in framboids can be evaluated by considering a theoretical system in which the concentration of monomers in the bulk solution, c_b, is constant. The concentration at the particle surface is c_0, the equilibrium concentration. The rate of increase in particle radius, r, with time, t, is then

$$dr/dt = [\mathcal{D}(1 + r/\delta)\, \nu_0(c_b-c_0)/r]/ [1+\mathcal{D}\,(1 + r/\delta)/kr]. \quad (1)$$

where $\mathcal{D}$ is the diffusion coefficient, δ is the width of the diffusion boundary layer around the particle, ν_0 is the molar volume of the monomer and k is the rate constant for the interface reaction. In a surface reaction controlled process, the interface reaction becomes rate controlling ($\mathcal{D} >> k$) the rate of growth is independent of particle size. In the diffusion-limited reaction ($\mathcal{D} << k$) the growth rate is a function of the particle size: as the particle size increases the growth rate decreases. Therefore diffusion-controlled growth has a much stronger tendency to produce the type of monodispersed microcrystals observed in framboids.

The result of the application of the LaMer model to framboid formation is that the time of formation of framboids can be estimated as the time from the point of burst nucleation to the point at which further crystal growth is negligible. The rate of surface growth of pyrite crystals at STP (25^{o}C, 0.1 MPa) is not well constrained but it

appears to be relatively rapid (Harmandas et al., 1998) and the time for framboid formation is limited by the diffusion of nutrients from the surrounding environment.

2.2 Length of time to form a framboid.

Rickard and Luther (2007) showed that the solubility of pyrite in aqueous solutions could be described in terms of the concentrations of Fe(II) and S(-II). The reason for this is the extremely fast kinetics of the equilibration of species such as FeS^0, S_2^{2-}, HS^- and H_2S and the extremely low solubility of pyrite. This means that there is a continuous supply of the key species for pyrite formation in sulfide solutions.

Since the kinetics of mackinawite, FeS_m, formation are extremely fast, the concentration of dissolved Fe and S in solution at STP is limited by the solubility of mackinawite, FeS_m, This is constant at pH > 6 and is equivalent to approximately 10^{-6} M FeS^0 at pH > 6 (Rickard, 2006). This means that the maximum dissolved concentration of Fe (II) + S(-II) available for pyrite formation in most natural aqueous solutions is 88 x 10^{-6} g L^{-1}.

A 10 μm diameter framboid has a mass of less than 2.6 x10^{-9} g. This is a maximum since the density of microcrystal packing varies according to its packing geometry (Rickard, 1970). In such a solution, the mass of pyrite in the 10 μm framboid will be contained in a volume of about 2.2 x 10^{10} μm^3 at a limiting dissolved Fe and S concentration of 10^{-6} M. This is equivalent to a sphere of solution with the framboid at its center with a radius of about 1600 μm.

In the framboid-forming system the limiting bulk solution in the sediment or water column can be regarded as approaching a constant value (cf. Rickard and Luther,

2007). This means that the rate of formation of the framboids can be closely approximated by a steady state solution to the three-dimensional equation for spherical diffusion (Berner, 1971; Lasaga, 1998; Raiswell et al., 1993; Rickard, 1973). If the diffusion coefficient, $\mathcal{D}$, is in $\mu m^2\ s^{-1}$, the framboid diameter, D, and the radius of the bulk solution containing the necessary dissolved iron and sulfide, R_b are in μm, the concentration of dissolved iron and sulfide in the bulk solution, c_b , and at the pyrite surface, c_0, are in moles μm^{-3} and the porosity, φ, is dimensionless then the flux, J, has units of g $\mu m^{-2}\ s^{-1}$, and can be described by equation (2).

$$J = 2\varphi\mathcal{D}\ R_b\ (c_b - c_0)/\ D\ (R_b - D/2). \quad (2)$$

which can be simplified to

$$J = \varphi\mathcal{D}\ R_b\ (c_b - c_0)/\ D/2\ (R_b - 1). \quad (3)$$

The flux can be modified to give the amount of material diffusing across the framboid boundary, J_s, by dividing J by A, the surface area of the framboid.

Then $A = \pi D^2$ and equation (3**)** becomes

$$J_s = 2\varphi\ \pi\ D\ \mathcal{D}\ R_b\ (c_b - c_0)/\ (R_b - 1). \quad (4)$$

equation (4**)** can be further simplified since pyrite is relatively insoluble and $c_b >> c_0$ so that

$c_b - c_0 \sim c_b$

and

R_b, in μm, is far greater than 1 so that

$R_b - 1 \sim R_b$

Equation (4) then becomes

$$J_s = 2\varphi \pi \mathcal{D} D c_b. \quad (5)$$

Equation (5) is interesting since it suggests that, within the precision of the system, the flux of dissolved nutrients to the framboid is independent of the radius of the bulk solution. Sensitivity analysis shows that the errors in this approximation are within the third decimal place of the exponential.

In sediments, diffusion is represented by the whole sediment diffusion coefficient $\mathcal{D}_s$ which takes into account the tortuosity Θ, a measure of the actual path length of the diffusion process (Berner, 1971). Then

$$\mathcal{D}_s = \mathcal{D} / \Theta^2. \quad (6)$$

and, since $\Theta > 1$, $\mathcal{D}_s < \mathcal{D}$. Values of the diffusion coefficient in sediments would be further reduced by cation exchange with mainly negatively charged clay particles, so that the apparent diffusion coefficient for positively-charged ions such as Fe^{2+} is far lower than might be expected from equation (6) whereas the value for negatively charged ions may more closely approximate to $\mathcal{D}_s$.

In the model the formation of framboids is diffusion-limited. Then $\mathcal{D}$, in equation (6) is the largest diffusion coefficient for Fe or S species in solution: the largest diffusion coefficient of the dissolved species limits the maximum flux. Various suggestions for the value of $\mathcal{D}_s$ have been published but the variation is relatively insignificant compared with uncertainties in other areas of the diffusion equation. Boudreau (1996) suggested $\mathcal{D} = (3.31 + 0.15T) \times 10^{-6}$ (where T is ^{o}C) in pure water which converts to $\mathcal{D}_s$ (Fe^{2+}) = 3.53 x 10^{-6} cm^2 s^{-1} in the first 30 cm of marine sediments (Raiswell and Anderson, 2005).

The porosity, φ, varies from 0.2 for a fine-grained clastic sediment to 1 for open water. With these parameters the flux, J, is 2.66 x 10^{-15} g FeS_2 s^{-1} and the 10 μm framboid will form within 11 days in open water. Note that in a fine-grained clastic sediment with φ = 0.2 the time will be extended to around 14 days. The sum effect of φ in equation (5**)** is that framboids form faster in the water column than in sediments.

3 Results

The time taken for framboids to form at STP (Fig. 3) is derived from the solutions to equation (5) for the flux, J_s (g μm^{-2} s^{-1}), to the framboid surface for various values of the framboid diameter. The framboid formation time is the period between burst nucleation and the final assembly of the microcrystals into the complete framboid.

Secondary internal structural reorganization may continue in some framboids over a period of time after aggregation (e.g. Wang et al., 2018) but this is not considered as part of the framboid formation time. The computations are for the limiting conditions where (a) the concentration of dissolved Fe and S in the bulk solution is controlled by the solubility of FeS_m (mackinawite) and (b) the density of the framboid is equivalent to that of a solid pyrite sphere with the framboid diameter. Both these are maxima but work in opposite directions. Thus if the concentrations of dissolved Fe and S in the bulk are less than the solubility product of FeS_m, then the formation time will be longer. By contrast, the actual density of pyrite in a framboid depends on the packing geometry of its constituent microcrystals and will be up to 20% less than the density of solid pyrite. This means that the framboid formation time will be less than the computed time. The net result of these approximations is that the computed value for the framboid formation time is accurate to within a magnitude.

[Figure 3]

Raiswell and Berner (1985) divided framboids into two groups: syngenetic (those formed within the water column) and diagenetic (those formed within the sediments). The time taken to form each of these types of framboid is shown in figure 4. Diagenetic framboids are assumed to form within fine-grained clastic sediments with typical porosities of around 20%. The range of framboid diameters is limited at a minimum of 2 μm and a maximum of 80 μm. Most framboids are within this size range but rare framboids have been reported with diameters >80 μm. However, the exponential nature of the curves suggests that these larger framboids will not take

significantly longer to form than the 80 μm framboids: the time taken is measured in years. For example the largest framboid reported in the literature (Sweeney and Kaplan, 1973) is 250 μm in diameter and this took around 3 years to form. By contrast an 80 μm diameter framboid would take about 2.2 years to form. In the natural environment the maintenance of steady state in dissolved Fe and S supply over relatively large distances in a biologically-active sediment for periods of over a year is likely to be uncommon and large framboids are consequently less abundant.

[Figure 4]

The mean size of sedimentary framboids is ~ 6 μm and they formed within about 5 days [Fig. 4]. The mean diameter of modern syngenetic framboids is 5 μm (recalculated from Wilkin et al, 1996) and these formed more rapidly, in about 3 days. The markedly shorter formation time for syngenetic framboids is due to a combination of their smaller sizes and the larger effective diffusion coefficients for dissolved components in water compared to sediments in sediments.

The smaller mean diameters of syngenetic framboids have been widely used as a proxy for the oxygenation state of paleo-water columns. In particular, researchers have used framboid sizes to probe the framboid populations for potential signatures of ancient euxinia. These syngenetic framboids form mainly at the redoxcline within the water column and their settling rates vary as the square of their radii. This means that potentially, the time available for framboid growth within the redoxcline is inversely proportional to their size and the formation of larger syngenetic framboids is less favored.

Although pyrite framboids can be formed at any stage during sediment evolution, most framboids are formed during the earliest stages of diagenesis. Calculations based on sedimentation rates have suggested bulk framboid formation mainly completed within about 5 years (Schieber and Schimmelmann 2007; Wilkin et al. 1996). This time period encompasses the computed formation times for all framboids, even the largest reported.

[Figure 5]

Measurements of groups of actual framboids show that formation times can be relatively homogeneous. Figure 5 shows that 9 of the 14 framboids in figure 1 formed over about 11 days. One formed in just 4 days and the largest took 33 days to form. The different framboid sizes reflect the relative chemical and physical stability of the local sites: the larger framboids form in sites with a longer period of time available for diffusive nutrient supply to occur. Trace and isotopic analyses of these framboids would thus reflect the chemistry of an instant of 30 million-year -old time. If it is assumed that a group of framboids, such as the one illustrated in figure 1, represents the same event, then the different framboid formation times provide a potential relative history of the sediment biogeochemistry at exceptionally high precision, diurnal scales.

The common occurrence of groups of framboids, such as those in figure 1, in sediments or within fossils has previously been problematic to explain. In extreme examples, framboids are observed in spheroidal clusters sometimes called polyframboids (Love, 1971) or *Rogenpyrit* (Fabricius, 1961). If each framboid

required a given volume of solution in which to form then we might expect to see framboids distributed at a distance from each other dependent on the size of the system necessary to contain the mass of dissolved Fe and S contained within the framboid. A feature of the model is that the rate of formation is independent of the size of the framboid-forming system, which is consistent with the observation of framboids commonly occurring in groups. In fact, burst nucleation only depletes a solution volume similar to that of the individual framboid. Subsequent pyrite crystal growth is relatively rapid and determined by the diffusion gradient caused by the difference between the extremely low solubility of pyrite and the concentrations of dissolved iron and sulfur in the bulk solution.

This model consistent with the common occurrence of pyrite framboids within dead organisms and fossils, such as shells and plant remains. Framboid formation is independent, for example, of the shell volume. Once the critical supersaturation for pyrite is reached at points within the shell, the size of the shell itself – which effectively constitutes the volume of the bulk solution in the model - is irrelevant

The relative short mean time for framboid formation of around 5 days is consistent with the common observation of pyrite framboids being formed within plant and animal cells before they have begun to deform on burial and during the earliest stages of cellular lysis when the broad structure of the cells are still intact.

4 Conclusions

Pyrite framboid formation involves the LaMer process of burst nucleation within a diffusion –limited regime. The consequence of the combination of burst nucleation,

extreme critical supersaturations and the diffusion –limited regime is that the time taken for pyrite framboid formation in sediments can be calculated.

The results show that sedimentary pyrite framboids take around 5 days to form on average. Rare larger framboids (≥ 80 μm in diameter) take years to form whereas smaller syngenetic framboids average 3 days. The relative short time required to form smaller framboids in the water column is consistent with the development of populations of small framboids in euxinic environments, where the time available for framboid formation is relatively limited through the influence of advection and the Stoke's law settling velocities of denser pyrite particles.

The sizes of the framboids are time-dependent and might be used to probe the evolution of the sedimentary environment at exceptionally high precision, diurnal scales.

Acknowledgements

I thank Alan Channing who asked the question. Rob Raiswell and Rick Wilkin reviewed an earlier draft and their detailed comments did much to improve the paper. TU Delft, Holland, provided the framboid sample imaged by Arnold Kruize in figure 1.

4.1 Competing financial interests

The author declares that he has no competing financial interests unfortunately.

References

Baronov, A., Bufkin, K., Shaw, D. W., Johnson, B. L., and Patrick, D. L., 2015, A simple model of burst nucleation: Physical Chemistry Chemical Physics, v. 17, no. 32, p. 20846-20852.

Berner, R. A., 1971, Principles of chemical sedimentology, New Yorlk, NY, McGraw-Hill.

Boudreau, B. P., 1996, Diagenetic Models and their Interpretation, Berlin, Springer Verlag.

Daubrée, M., 1875, Examples of contemporary formation of iron-pyrites in thermal springs and in sea-water: Philosophical Magazine Series 4, v. 50, no. 334, p. 562-564.

Duckworth, R., Fallick, A. E., and Rickard, D., 1994, Mineralogy and sulfur isotope composition of the Middle Valley massive sulfide deposit, northern Juan de Fuca Ridge: Proceedings of the Ocean Drilling Program, v. 139, p. 373-378.

Fabricius, F., 1961, Die Strukturen des "Rogenpyrits" (Kossener Schichten, rat) als Beitrag zum Problemen der "Veretzen Bakterien". Geologische Rundschau, v. 51, p. 647-657.

Guy, B. M., Beukes, N. J., and Gutzmer, J., 2010, Paleoenvironmental controls on the texture and chemical composition of pyrite from nonconglomeratic sedimentary rocks of the Mesoarchean Witwatersrand Supergroup, South Africa: South African Journal of Geology, v. 113, no. 2, p. 195-228.

Hallbauer, D. K., 1986, The mineralogy and geochemistry of the Witwatersrand pyrite, gold, uranium and carbonaceous matter., *in* Anhaeusser, C. R., and Maske, S., eds., Mineral Deposits of Southern Africa., Geological Society of South Africa, p. 731-752.

Harmandas, N. G., Navarro Fernandez, E., and Koutsoukos, P. G., 1998, Crystal growth of pyrite in aqueous solutions. Inhibition by organophosphorus compounds: Langmuir, v. 14, no. 5, p. 1250-1255.

Kanehira, K., and Bachinski, D., 1967, Framboidal pyrite and concentric textures in ores of the Tilt Cove Mine, Northeastern Newfoundland: Canadian Mineralogist, v. 9, p. 124-128.

Kashchiev, D., 2011, Note: On the critical supersaturation for nucleation: Journal of Chemical Physics, v. 134, no. 19.

Lamer, V. K., 1952, Nucleation in phase transitions: Industrial and Engineering Chemistry, v. 44, no. 6, p. 1270-1277.

Lamer, V. K., and Dinegar, R. H., 1950, Theory, production and mechanism of formation of monodispersed hydrosols: Journal of the American Chemical Society, v. 72, no. 11, p. 4847-4854.

Large, D. J., Fortey, N. J., Milodowski, A. E., Christy, A. G., and Dodd, J., 2001, Petrographic observations of iron, copper, and zinc sulfides in freshwater canal sediment: Journal of Sedimentary Research, v. 71, no. 1, p. 61-69.

Lasaga, A. C., 1998, Kinetic theory in the Earth sciences, Princeton, NJ, Princeton University Press, 811 p.:

Love, L., and Amstutz, G. C., 1969, Framboidal pyrite form two andesites: Neues Jahrbuch fur Mineralogie, Geologie und Palaontologie, v. 3, p. 97-108.

Love, L. G., 1971, Early diagenetic polframboidal pyrite ,primary and redeposited, form the Wenlockian Denbigh Grit Group, Conway, North Wales, U.K.: Journal of Sedimentary Petrology, v. 41, p. 1038-1044.

MaClean, L. C. W., Tyliszczak, T., Gilbert, P., Zhou, D., Pray, T. J., Onstott, T. C., and Southam, G., 2008, A high-resolution chemical and structural study of framboidal pyrite formed within a low-temperature bacterial biofilm: Geobiology, v. 6, no. 5, p. 471-480.

Ohfuji, H., and Akai, J., 2002, Icosahedral domain structure of framboidal pyrite: American Mineralogist, v. 87, no. 1, p. 176-180.

Ohfuji, H., Boyle, A. P., Prior, D. J., and Rickard, D., 2005, Structure of framboidal pyrite: An electron backscatter diffraction study: American Mineralogist, v. 90, no. 11-12, p. 1693-1704.

Ohfuji, H., and Rickard, D., 2005, Experimental syntheses of framboids - a review: Earth-Science Reviews, v. 71, no. 3-4, p. 147-170.

Ohfuji, H., Rickard, D., Light, M. E., and Hursthouse, M. B., 2006, Structure of framboidal pyrite: a single crystal X-ray diffraction study: European Journal of Mineralogy, v. 18, no. 1, p. 93-98.

Papunen, H., 1966, Framboidal texture of the pyrtitic layer found in a peat bog in SE-Finland: Comptes Rendus de la Societe geologique de Finlande, v. 38, p. 117-125.

Perry, K. A., and Pedersen, T. F., 1993, Sulfur speciation and pyrite formation in meromictic ex-fjords: Geochimica Et Cosmochimica Acta, v. 57, no. 18, p. 4405-4418.

Raiswell, R., and Anderson, T. F., 2005, Reactive iron enrichment in sediments deposited beneath euxinic bottom waters: Constraints on supply by shelf recycling, Geological Society Special Publication, Volume 248, p. 179-194.

Raiswell, R., and Berner, R. A., 1985, Pyrite formation in euxinic and semi-euxinic sediments: American Journal of Science, v. 285, no. 8, p. 710-724.

Raiswell, R., Whaler, K., Dean, S., Coleman, M. L., and Briggs, D. E. G., 1993, A simple 3-dimensional model of diffusion-with-precipitation applied to localized pyrite formation in framboids, fossils and detrital iron minerals: Marine Geology, v. 113, no. 1-2, p. 89-100.

Read, R. A., 1968, Deformation and metamorphism of the San Dionisio pyritic ore body, Rio Tinto, Spain [PhD: Imperial College.

Rickard, D., 1970, The origin of framboids: Lithos, v. 3, p. 269-293.

-, 1973, Limiting conditions for sedimentary sulfide ore formation: Economic Geology, v. 68, p. 605-617.

-, 2006, The solubility of FeS: Geochimica et Cosmochimica Acta, v. 70, no. 23 SPEC. ISS., p. 5779-5789.

-, 2012, Sedimentary Pyrite, Developments in Sedimentology, Volume 65, p. 233-285.

-, 2015, Pyrite: A Natural History of Fool's Gold, New York, NY, OUP USA.

Rickard, D., and Luther, G. W., 2007, Chemistry of iron sulfides: Chemical Reviews, v. 107, no. 2, p. 514-562.

Rickard, D., 1969, The microbiological formation of iron sulfides: Stockholm Contrib. Geol., v. 20, p. 49-66.

Rickard, D., and Zweifel, H., 1975, Genesis of Precambrian sulfide ores, Skellefte District, Sweden: Economic Geology, v. 70, no. 2, p. 255-274.

.

Ross, D. A., and Degens, E. T., 1974, Recent sediments of the Black Sea, *in* Degens, E. T., and Ross, D. A., eds., The Black Sea - Geology, chemistry and biology, Volume Memoir 20: Tulsa, Ok., American Association of Petroleum Geologists, p. 183-199.

Rust, G. W., 1931, Colloidal primary copper ores at Cornvall Mines, Southwestern Missouri: Journal of Geology, v. 43, p. 398 - 426.

Schoonen, M. A. A., and Barnes, H. L., 1991, Reactions forming pyrite and marcasite from solution .1. Nucleation of FeS2 below 100oC: Geochimica Et Cosmochimica Acta, v. 55, no. 6, p. 1495-1504.

Skei, J. M., 1988, Formation of framboidal iron sulfide in the water of a permanently anoxic fjord - Framvaren, South Norway: Marine Chemistry, v. 23, no. 3-4, p. 345-352.

Sweeney, R. E., and Kaplan, I. R., 1973, Pyrite framboid formation: Laboratory synthesis and marine sediments: Econ. Geol., v. 68, p. 618-634.

Vallentyne, J. R., 1963, Isolation of pyrite spherules from recent sediments: Limnology and Oceanography, v. 8, no. 1, p. 16-29.

Wang, J., Mbah, C. F., Przybilla, T., Zubiri, B. A., Spiecker, E., Engel, M., and Vogel, N., 2018, Magic number colloidal clusters as minimum free energy structures: Nature Communications, v.9, article number 5259.

Wang, Q., and Morse, J. W., 1996, Pyrite formation under conditions approximating those in anoxic sediments: I. Pathway and morphology: Marine Chemistry, v. 52, no. 2, p. 99-121.

Wilkin, R. T., and Barnes, H. L., 1997, Formation processes of framboidal pyrite: Geochimica Et Cosmochimica Acta, v. 61, no. 2, p. 323-339.

Wilkin, R. T., Barnes, H. L., and Brantley, S. L., 1996, The size distribution of framboidal pyrite in modern sediments: An indicator of redox conditions: Geochimica et Cosmochimica Acta, v. 60, no. 20, p. 3897-3912.

FIGURE CAPTIONS

Figure 1. Scanning electron micrograph of pyrite framboids from the Oligocene (28.1 -33.9 Ma) Rupel Clay Member, Netherlands. Photo: Arnold Kruize.

Figure 2. Elements of the LaMer theory for the formation of uniform colloidal particles. An initial induction period with insignificant nucleation rates is followed by a short period of burst nucleation (bn) where the rate increases exponentially followed by a growth dominated period where the formation of new nuclei is again insignificant.

Figure 3. Logarithm of time in seconds versus framboid size in μm for limiting conditions (see text) for water column and sediment at 25^{o}C and 0.1 MPa.

Figure 4. Linear plot of framboid size versus formation time in days for small syngenetic and diagenetic framboids

Figure 5. Time taken (in days) for the framboids in figure 1 to form.

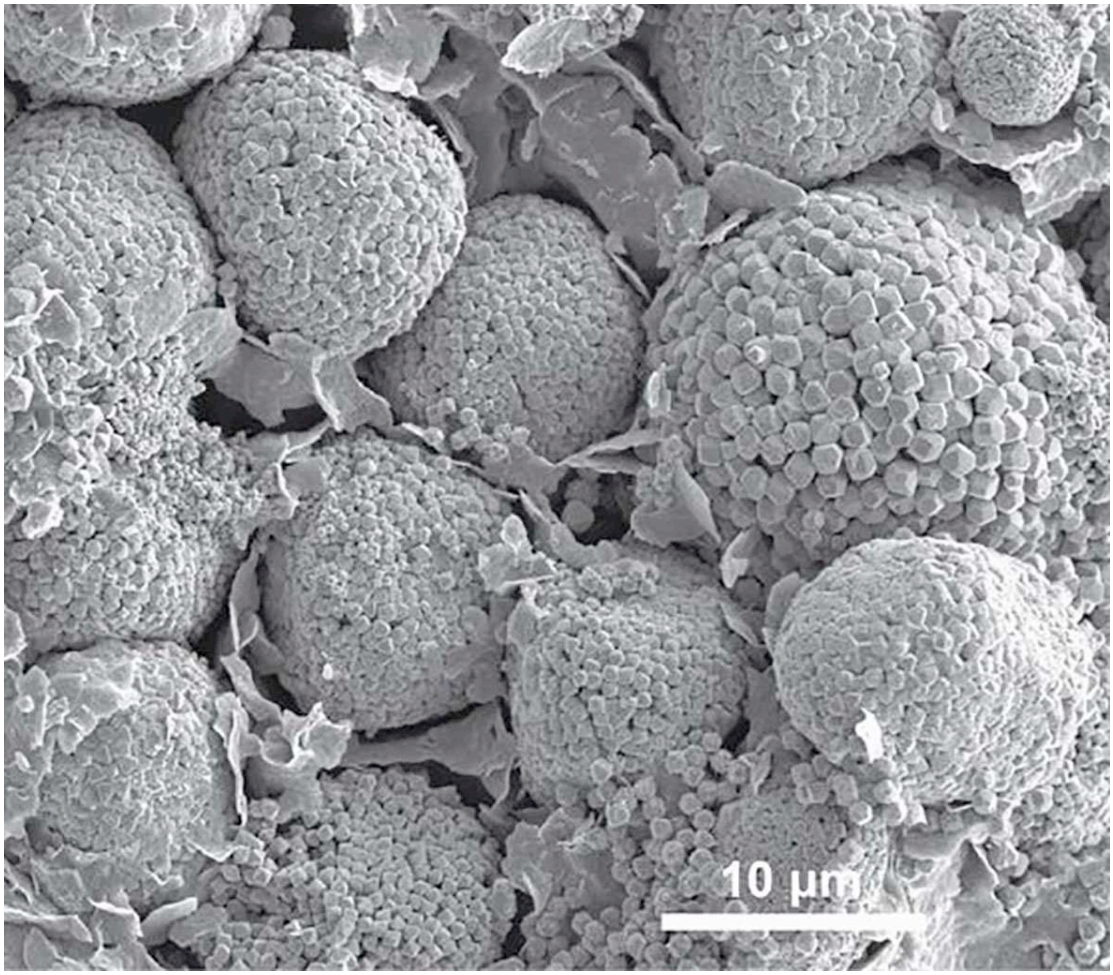

Fig. 1.

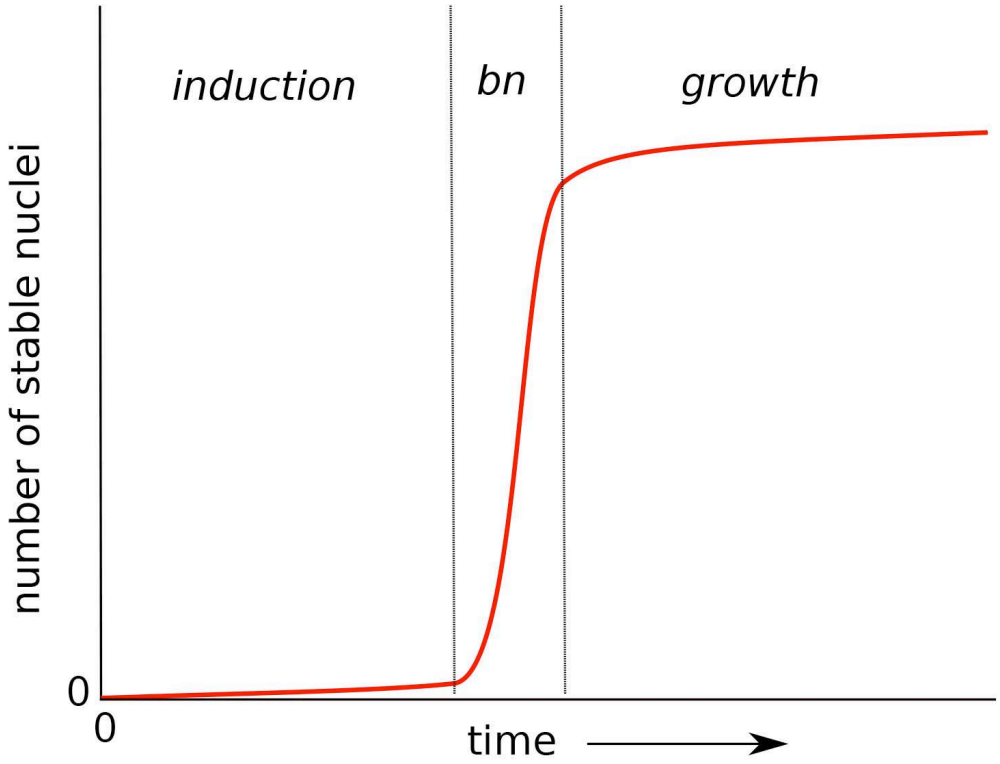

Fig. 2

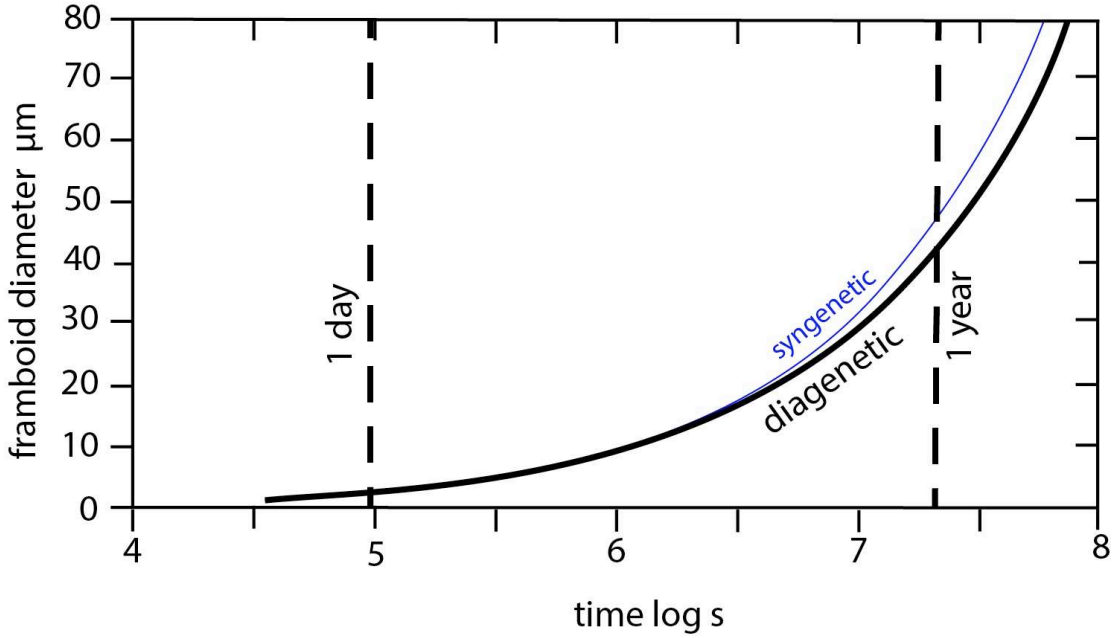
framboid diameter µm
80
70
60
50
40
30
20
10
0
4
5
6
7
8
time log s
1 day
1 year
syngenetic
diagenetic

Fig.3

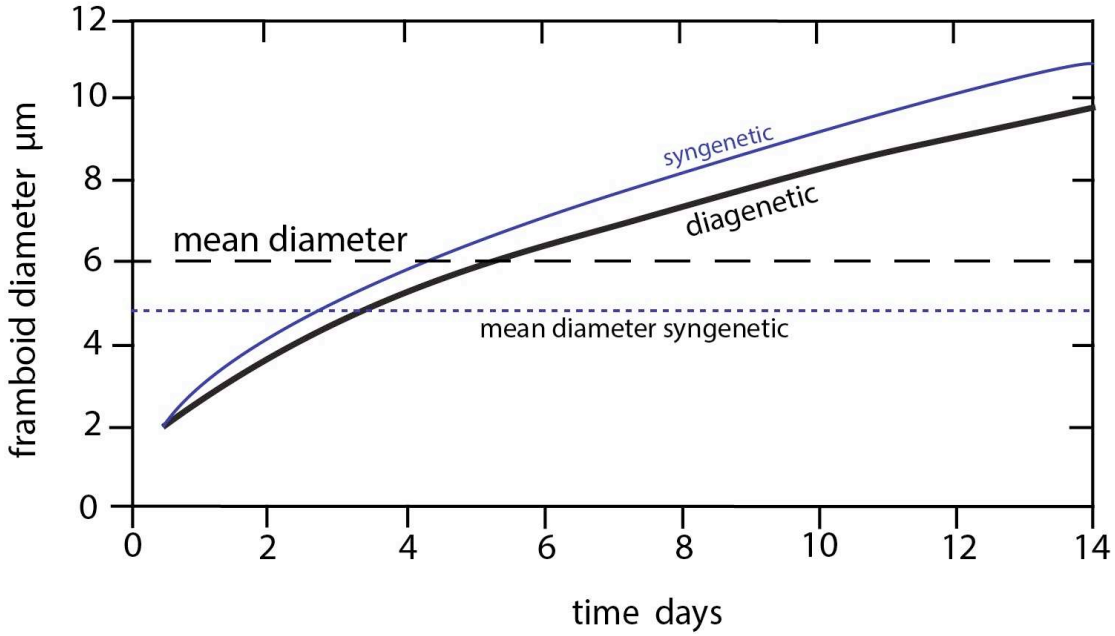
framboid diameter µm
time days
syngenetic
diagenetic
mean diameter
mean diameter syngenetic
0
2
4
6
8
10
12
14

Fig. 4

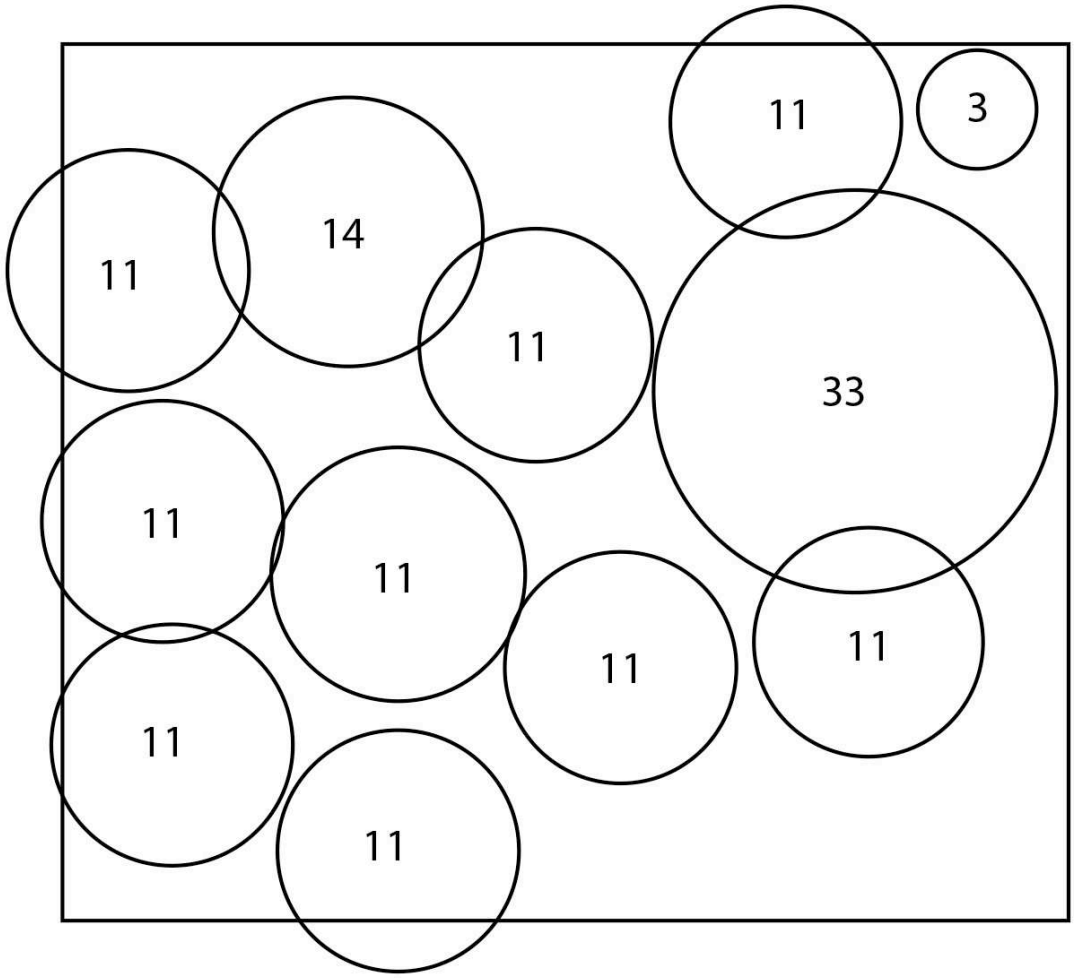

Fig .5.